NSG-1063

ELECTRON ENERGY DISTRIBUTIONS IN URANIUM HELIUM MIXTURES

by

MICHAEL ANTHONY MAKOWSKI

NUCLEAR ENGINEERING PROGRAM

UNIVERSITY of ILLINOIS at URBANA-CHAMPAIGN

URBANA, 1977

ELECTRON ENERGY DISTRIBUTIONS

IN URANIUM HELIUM MIXTURES

BY

MICHAEL ANTHONY MAKOWSKI
B.S., University of Illinois, 1975

THESIS

Submitted in partial fulfillment of the requirements
for the degree of Master of Science in Nuclear Engineering
in the Graduate College of the
University of Illinois at Urbana-Champaign, 1977

Urbana, Illinois

Abstract

The high-energy portion of the electron energy distribution for mixtures of uranium and helium at 1 atm, 5000°K, and a neutron flux of $2 \times 10^{12}/cm^2$-sec have been calculated. The addition of He improves the heat transport characteristics of the plasma and has the feature that the He energy levels lie in the high-energy portion of the electron distribution, potentially allowing non-maxwellian excitation. It is concluded, however, that the resulting reaction rates are marginal relative to achieving inversion in He.

ACKNOWLEDGMENT

The author wishes to thank Professor George H. Miley for his guidance and suggestions throughout the course of this work. The advice and discussions of Dr. Chan Choi and Ed Maceda are also greatly appreciated. Also deserving of thanks is my wife, Betty, for her continued moral support. Recognition is due the excellent secretarial staff in general and to Mrs. Jeri Borchers and Mrs. Carol Mathis in particular. The author is also grateful for the financial support of this work provided by NASA under Grant US NASA NSG 1063.

TABLE OF CONTENTS

Several schemes to do this have been suggested.[2] For example, the original application of the light-bulb reactor was as a rocket engine in which a supercooled liquid is rapidly heated.[3] As the liquid is heated it is turned into a gas and the expanding hot gas is then sent to a nozzle where it is used to propel the rocket.

Since then several other ideas have been suggested. One is H_2 production from water. H_2 has been proposed as a substitute for natural gas, the supply of which is rapidly being depleted. In most of the schemes for H_2 production a heat source on the order of 1000°C is required.[4,5] Others[6] require a radiation source to perform the chemical breakdown of water. Both of these sources, radiation and heat, are conveniently combined in a light-bulb reactor.

Another potential application is for nuclear pumped lasers.[7] This would be a form of direct energy conversion where the electrons excite one of the plasma species, causing it to lase. Laser energy represents a desirable source of energy because its monoenergetic nature makes a broad spectrum of applications possible.

Uranium plasmas themselves are of interest outside the realm of the reactor. For instance a uranium plasma could be used for laser isotope separation.[8] A laser pulse can be applied to a mixture of gaseous U-235 and U-238 such that preferential excitation or ionization of one of the species is obtained. The ions can then be collected by electric field methods. In the case of excited atoms, a second pulse can be used to ionize them. Separation factors of 26 to many thousands are theoretically possible by this method.[9]

Still other applications of the light-bulb reactor are its use as a high-level actinide waste burner and as a breeder of U-233 from thorium.[10,11]

II. REVIEW OF PREVIOUS WORK

Early work related to this topic was carried out by R. H. Lo[12] and B. S. Wang.[13] Their studies were concerned with the modeling of a radiation induced plasma. More exactly they sought the electron distribution due to a delta function source of high energy electrons. Noble gases were used as the background species instead of uranium since more experimental data was available as a check of the validity of the model. Lo approached the problem analytically and his results agreed well with both the experimental data available and with the Monte Carlo simulation of Wang.

This work was followed up by that of Bathke.[1] He developed an analytic model for a uranium plasma with a distributed high-energy electron source. He also developed a Monte Carlo code to check the validity of the analytic model. The two agree well within the limiting assumptions of the analytic model.

The area of study was broadened by E. Maceda[14] who worked on the radiation transport aspect of the plasma. His results indicate that population inversions in pure uranium are possible and that the type of radiation (frequency) eminating from the plasma may be modified by the choice of different seed gases.

The work of D. Suhre[15] is also important to the present effort. Suhre calculated the electron energy distribution in an N_2 gas due to a delta function source of high-energy electrons. This is significant since prior work had only considered atomic species. Suhre calculated analytically and measured experimentally the electron energy distribution. For low-energy electrons the distribution "dips" significantly in the region of 1 eV to 4 eV where the cross section for vibrational excita-

tion of N_2 by electron impact has a very large value ($\sim 10^{-16} cm^2$). Molecular species ultimately need to be considered in the case of UF_6 which is what this whole effort has been aimed at.

The work presented here essentially represents an extension of Bathke's[1] work to include a second species in addition to uranium.

III. MODEL

A. Cross Sections

Differential energy transfer cross sections must be used in the slowing down model used here. A formulation originally developed by Gryzinski[15] is used and is defined as follows:

$\frac{d\sigma(E,E')}{dE'}$ = the probability per unit energy that an electron of a given energy, E, losing an amount of energy, E'-E, in an excitation or ionization collision.

Evidently, if the differential cross section is integrated over all possible energy losses E', the total cross section for a given event results, i.e.

$$\int_0^\infty \frac{d\sigma(E,E')}{dE'}\, dE' = \sigma(E) \qquad (1)$$

This model makes the assumption that ionization and excitation collisions may be described as a collision between two free electrons. The atomic electron is assumed to have a constant velocity and be distributed isotropically about the nucleus. The treatment is thus classical, but quantum mechanical corrections are included.[17]

The results shown in Figs. 1 and 2 were obtained using modified Gryzinski cross for ionization and excitation of He and He^+ by electrons.

An experimental ionization cross section for He is plotted in Fig. 1 for comparison. The total cross section predicted by the Gryzinski model agrees well with the experimental data. Also shown is an experimental excitation cross section. Here the agreement between theory and experiment is not nearly so good. The experimental cross section exhibits no sharp peaking as does the theoretical curve. The

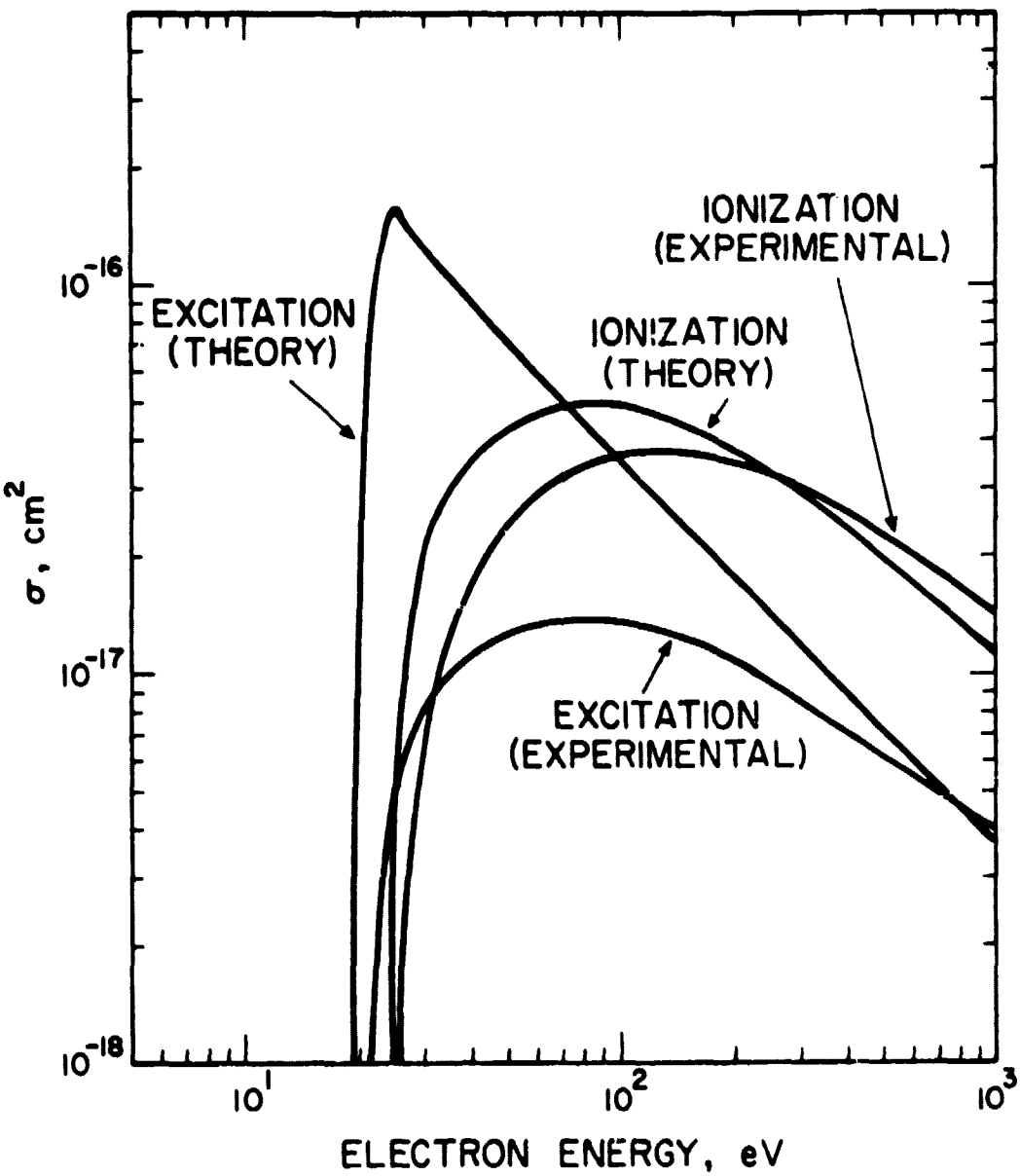

Fig. 1. Comparison of Ionization and Excitation Cross Sections from the Gryzinski Model and Some Experimental Data.

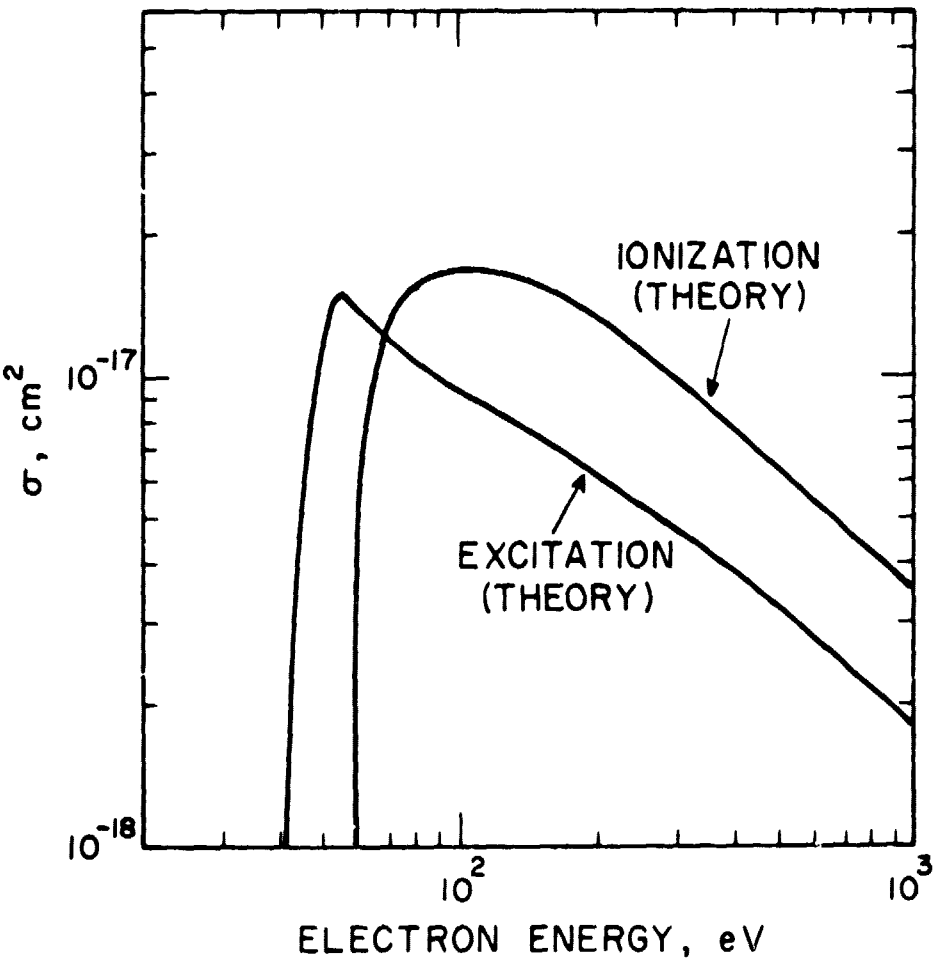

Fig. 2. Ionization and Excitation Cross Sections for He^+ from the Gryzinski Model.

situation is not as grim as it seems, however. The experimental curve is only a sum of three excitation cross sections for different states in He. It was not possible to include all states because data was not available. The sum of the missing cross sections for the other states could conceivably raise the total excitation cross section by 25%. In fact the lack of a sharp peak in the experimental cross sections could be explained by the missing n^3S, n^1d, and n^3d cross sections which exhibit this type of peaking behavior. Despite this if one assumes only a 25% increase in the experimental cross section, using the electron distribution for a 40% U-60% He mixture, the theoretical cross section predicts about 2.7 times the number of excitation found using the experimental curve. This is not considered to be too large a discrepency considering the lack of complete experimental data.

B. Slowing Down Model

The model used to find the electron distribution, f(E), is quite simple. It is derived by Bathke[1] and is:

$$f(E) = \frac{\int_E^\infty S(E')\, dE'}{\left(\frac{dE}{dt}\right)\Big|_E} \qquad (2)$$

where S(E') is the electron source rate and $\left(\frac{dE}{dt}\right)\Big|_E$ is the rate at which electrons deposit their energy in the background species via excitation, ionization, and coulomb collisions.

A rate of energy loss per collision may be thought of in the following terms:

$$\left(\frac{dE}{dt}\right)\Big|_E = \begin{pmatrix}\text{average}\\ \text{energy}\\ \text{loss per}\\ \text{collision}\end{pmatrix} \times \begin{pmatrix}\text{probability of}\\ \text{collision per}\\ \text{unit path}\\ \text{length}\end{pmatrix} \times \begin{pmatrix}\text{path length}\\ \text{traveled}\\ \text{per unit}\\ \text{time}\end{pmatrix} \quad (3)$$

The average energy loss per collision for an electron of energy E, $\langle E \rangle_{loss}$, may be computed from the differential energy transfer cross section as follows:

$$\langle E \rangle_{loss} = \frac{\int_0^\infty E' \frac{d\sigma(E,E')}{dE'} dE'}{\int_0^\infty \frac{d\sigma(E,E')}{dE'} dE'} = \frac{1}{\sigma(E)} \int_0^\infty E' \frac{d\sigma(E,E')}{dE'} dE'. \quad (4)$$

The probability of collision per unit path length for a given type of interaction is simply the macroscopic cross section for that type of collision, i.e. $\sum(E) = n \cdot \sigma(E)$ where n is the density of the background species with which the electrons interact. Finally, the path length traveled per unit time is the velocity of the electron, v. Hence, Eq. (3) becomes

$$\left(\frac{dE}{dt}\right)\Big|_E = \langle E \rangle_{loss} \sum(E)\, v \quad (5)$$

$$= nv \int_0^\infty E' \frac{d\sigma(E,E')}{dE'} dE' \quad (6)$$

Equation (6) may be used to calculate the rate of energy loss per excitation or ionization collision. However, for coulomb collisions other expressions must be used which are readily available in the literature. One such expression is[18]:

$$\left\langle \frac{dE}{dt} \right\rangle = - \frac{4\pi e^2}{v} \sum_i L\, n_i\, e_i^2 \left[\frac{\Phi(b_i v)}{m_i} - \frac{2 b_i v (m+m_i)}{m m_i \sqrt{\pi}} e^{-b_i^2 v^2} \right] \qquad (7)$$

where

$\sum_i$ indicates a sum over all background species

L = coulomb logarithm $\tilde{\sim} 20$

$b_i = (m_i/2T_i)^{\frac{1}{2}}$

m = mass of an electron; m_i = mass of species i

v = velocity of the electron

$$\Phi(x) = 1 - \frac{2}{\sqrt{\pi}} \int_x^\infty e^{-\xi^2}\, d\xi.$$

The total rate of energy loss by the electrons is taken as the sum of the individual loss processes, i.e.

$$\left(\frac{dE}{dt}\right)_{\text{total}} = \left.\frac{dE}{dt}\right|_{\substack{\text{coulomb} \\ \text{collisions}}} + \left.\frac{dE}{dt}\right|_{\substack{\text{excitation} \\ \text{collisions}}} + \left.\frac{dE}{dt}\right|_{\substack{\text{ionization} \\ \text{collisions}}} \qquad (8)$$

There are two sources of electrons. The primary electrons arise from the stripping of fission fragments in the fission of an atom of U-235. This source accounts for the majority of the high-energy electrons. The secondary electrons are created by ionization collisions between the primary electrons and background species. These secondary electrons may be thought of as a perturbation to the primary source. The primary source of electrons may be calculated by integrating the fission fragment distribution over the differential energy transfer cross section for ionization. A first guess for the high-energy tail is obtained by use of Eq. (2).

The secondary electron source is obtained in a similar fashion, the only difference being that now the differential energy transfer cross

section for ionization is integrated over the first guess electron distribution. This secondary source is then added to the primary source and a new distribution function is obtained. The procedure of integrating the distribution over the ionization cross section to obtain a new source which is in turn used to calculate a new distribution function is repeated until the process converges to the final distribution function.

C. Model for the Distribution Itself

The electron distribution itself is assumed to be the superposition of a Maxwellian distribution of thermalized electrons and a high-energy tail described by Eq. (2). The assumption and validity of a Maxwellian will be discussed below. The derivation of Eq. (2) also requires various assumptions including

a) A steady-state plasma and an infinite media

b) A homogeneous mixture of U-235 and He

c) Continuous slowing down of electrons

d) Negligible recombination of electrons with background species

e) Negligible upscattering.

Assumptions a) and b) serve to define and simplify the problem under study. Since the energy losses involved in ionization, excitation, or coulomb collisions are small in comparison to the energy of the primary electron, continuous slowing down of electrons is assumed. However, the assumption rapidly breaks down on the low-energy end of the high-energy tail where the electron energy is comparable to excitation and ionization energies of helium and uranium. In comparison to a more exact Monte Carlo calculation by Bathke[1] it may be seen that the model is not

seriously in error. Recombination of electrons with background species is ignored since the energetic electrons stripped from the fission fragments will not recombine until they have sufficiently slowed down. The energy at which this process typically takes place is out of the domain under consideration. Upscattering is negligible for the same reason. Note that these assumptions apply only to the calculation of the high-energy tail. The only loss mechanism for high-energy electrons is down scattering to thermal energies.

IV. RESULTS

A. Distribution Obtained

The distribution is assumed to be a superposition of a Maxwellian and a high energy tail. Since the bulk of the electrons are in thermal equilibrium described by the Maxwellian the Saha equation may be used to predict the initial densities of the plasma constituents.

The electron density is important in calculating the $\frac{dE}{dt}$ due to coulomb collisions. The Saha density of the electrons is used for an initial guess for n_e. Thus, the primary and secondary electrons produced by ionization of background species are considered perturbations to the Saha density and are added to it.

In the calculation of the Saha densities it is assumed that one in 10^4 helium atoms exist in the metastable state. This figure was arrived at by an excited state density calculation performed by Maceda[19] using Lo's distribution for He gas at 300°K. Although the distribution functions obtained in this calculation and those of Lo are quite similar, a major difference between them is the gas temperature. The temperatures in this calculation are over an order of magnitude greater than the plasma temperature from which the one in 10^4 helium atoms in the metastable state figure was obtained. However, this figure is thought not to be in serious error and it is used as a first approximation for the number of He-metastables. To arrive at a more accurate number, an iterative scheme must be employed. The metastable density is initially guessed at and the distribution function is then calculated. Given the distribution, an excited-state-density calculation may be performed yielding a new He-metastable density. This new He metastable density

may then be used to recalculate the distribution function, and so on until the process converges to the final distribution.

Any error introduced by assuming the ratio $1:10^4$ is certainly negligible for uranium concentration greater than 10% since the dominant contribution to the electron population is from uranium. This is clearly seen in Fig. 4 which shows a plot of electron density versus the partial pressure of uranium. The electron density falls off linearly with P_u/P_{tot} until a concentration of about 10% uranium is reached. Beyond that point the electron density falls off rapidly. The assumed ratio might only be seriously in error for extremely low uranium concentrations (< .1%).

In Fig. 3 the He^+ density is seen to have a broad maximum at ~3500°K and then starts to decrease slightly. This occurs because at ~3500°K a significant portion of the He-metastables begin to ionize and as the temperature increases beyond this point virtually all of the metastables ionize. At higher temperatures (>4000°K), virtually all the He-metastables have been ionized. Since the He-metastable density is initially assumed to be a constant fraction of the total number of He atoms at any given temperature, and for high temperatures all of the He-metastables become ionized, the He^+ curve should follow the He curve at high temperatures. This is indeed what happens and since the He density decreases with temperature so does the He^+ density.

The above trends for He and He^+ are borne out in Fig. 5 which displays the ionization fraction of both He and U versus temperature. The ratio of He^+ to He saturates at 10^{-4} corresponding to the fraction of He initially assumed to be in the metastable state.

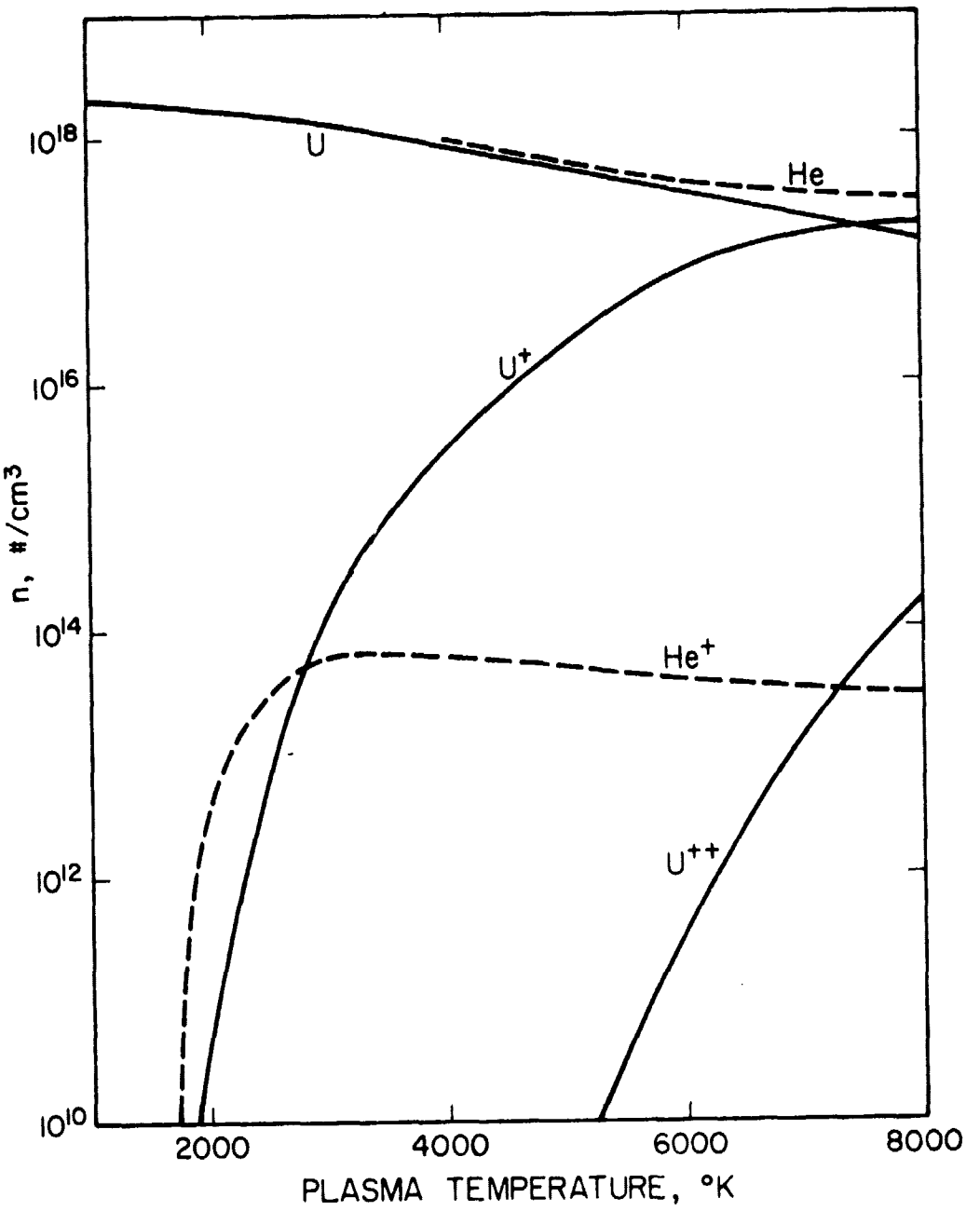

Fig. 3. Saha Densities at One Atmosphere vs. Temperature for a Mixture of 50% U and 50% He.

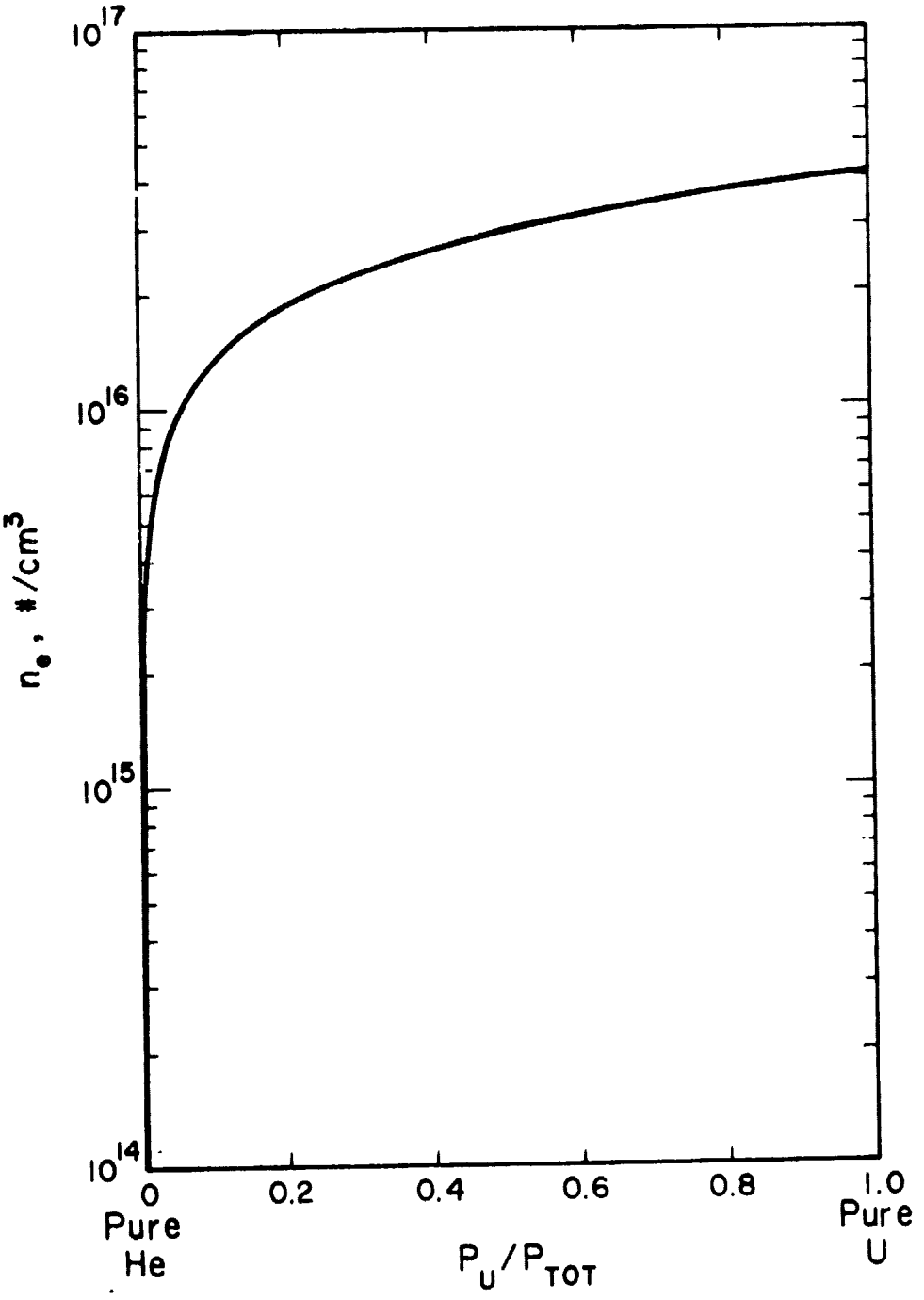

Fig. 4. Electron Density, n_e, vs. Partial Pressure of U at 5000°K.

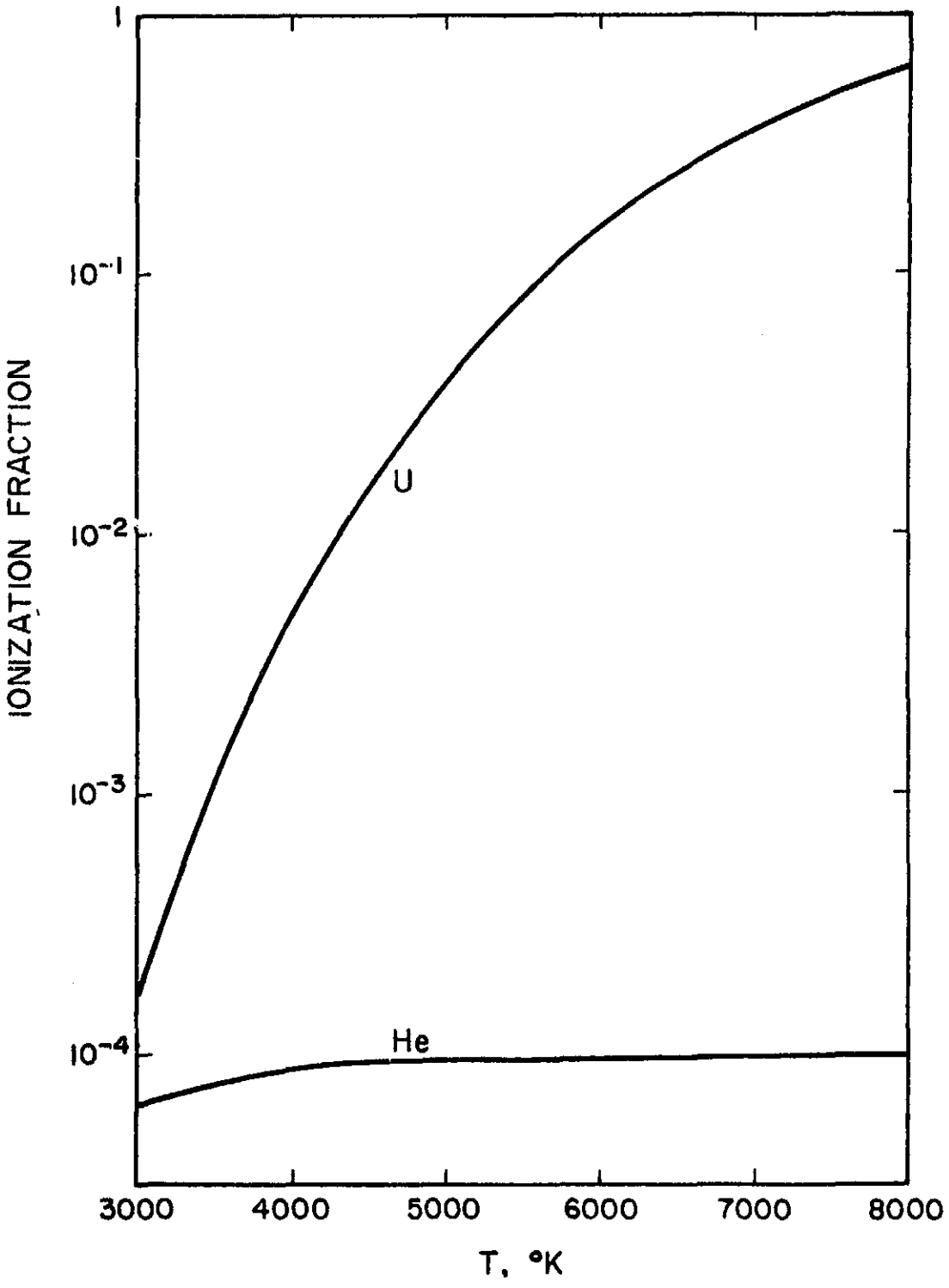

Fig. 5. Ionization Fraction of He and U vs. Temperature.

Figure 6 shows the distribution function obtained for various partial pressures of U for a plasma temperature of 5000°K and a neutron flux of $2 \times 10^{12}/cm^2$-sec. The curves are normalized with respect to power, i.e., the power output from the entire plasma is the same in all cases. Since the neutron flux is the same in all cases and power is proportional to the neutron flux and the uranium concentration, constant power requires the volume of the plasma to increase. The results scale linearly with neutron flux[1].

Several trends are evident in Fig. 6. One is that the magnitude of the high-energy tail decreases as the uranium concentration decreases. This is due to the increased stopping power, $\left(\frac{dE}{dx}\right)$ of the plasma caused by the increased concentration of helium. A sharp drop in the high-energy tail at ~20 eV is quite prominant for low uranium concentrations. This drop corresponds to the peak of the He cross sections and is again associated with the stopping power which in this case undergoes a step change near the energy at which the He cross sections peak. Also shown for reference are typical states of U and He. Note that the He^+ states lie in the high-energy tail of the distribution.

Figure 7 shows the high-energy tails of Fig. 6 in greater detail. The Maxwellian for 100% U is drawn in for reference. It should be noted that the point of intersection of the thermal background described by the Maxwellian and the high-energy tail is not well defined. The electron density in this energy range (10 eV to 18 eV) is quite small in comparison to the total electron population and the cross section for excitation and ionization of uranium are quite large. Hence, even small perturbations could easily cause a deviation from the assumed Maxwellian.

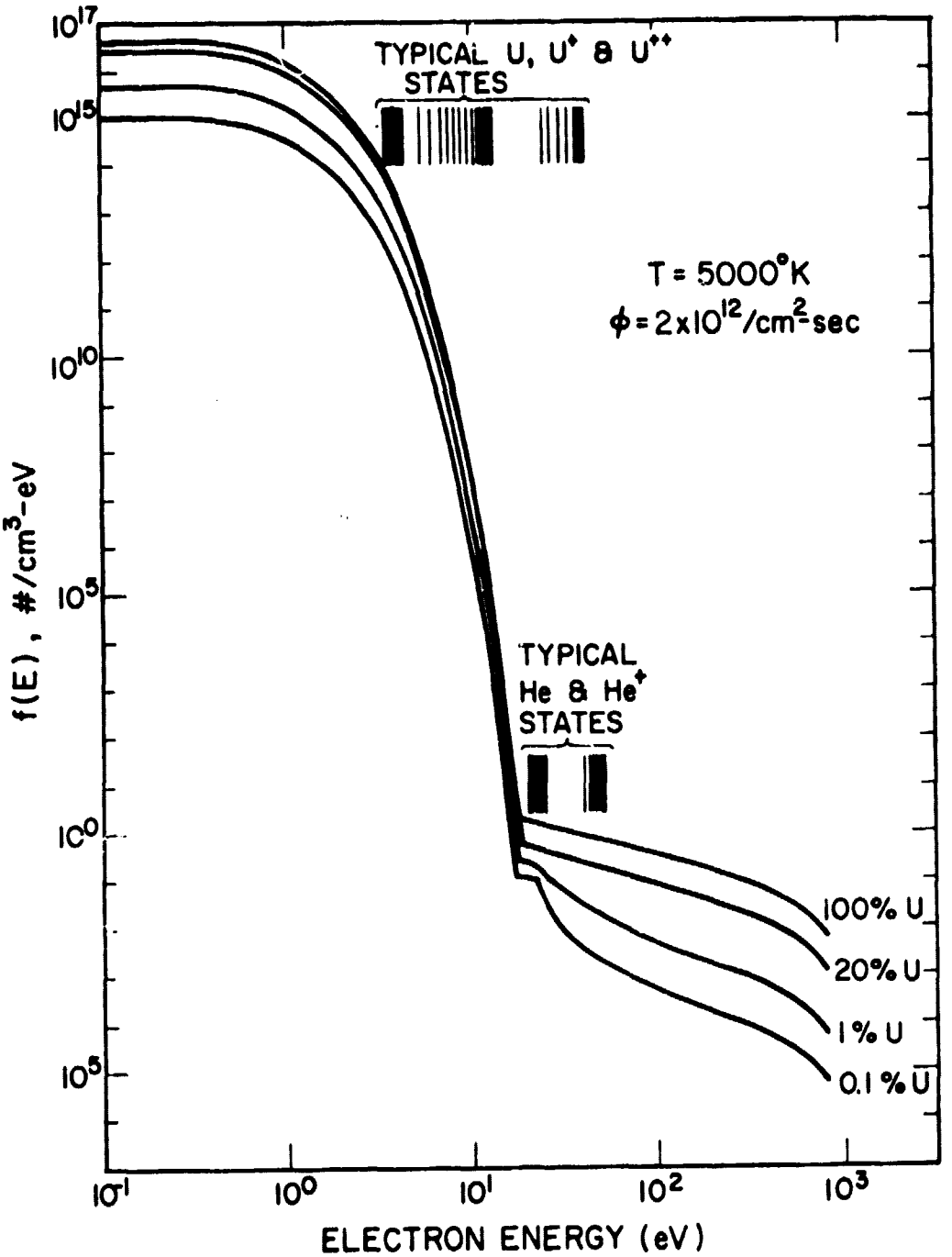

Fig. 6. Distribution Function for Different Partial Pressures of U for a Plasma Temperature of 5000°K and a Neutron Flux of 2 x 10^{12}/cm^2-sec.

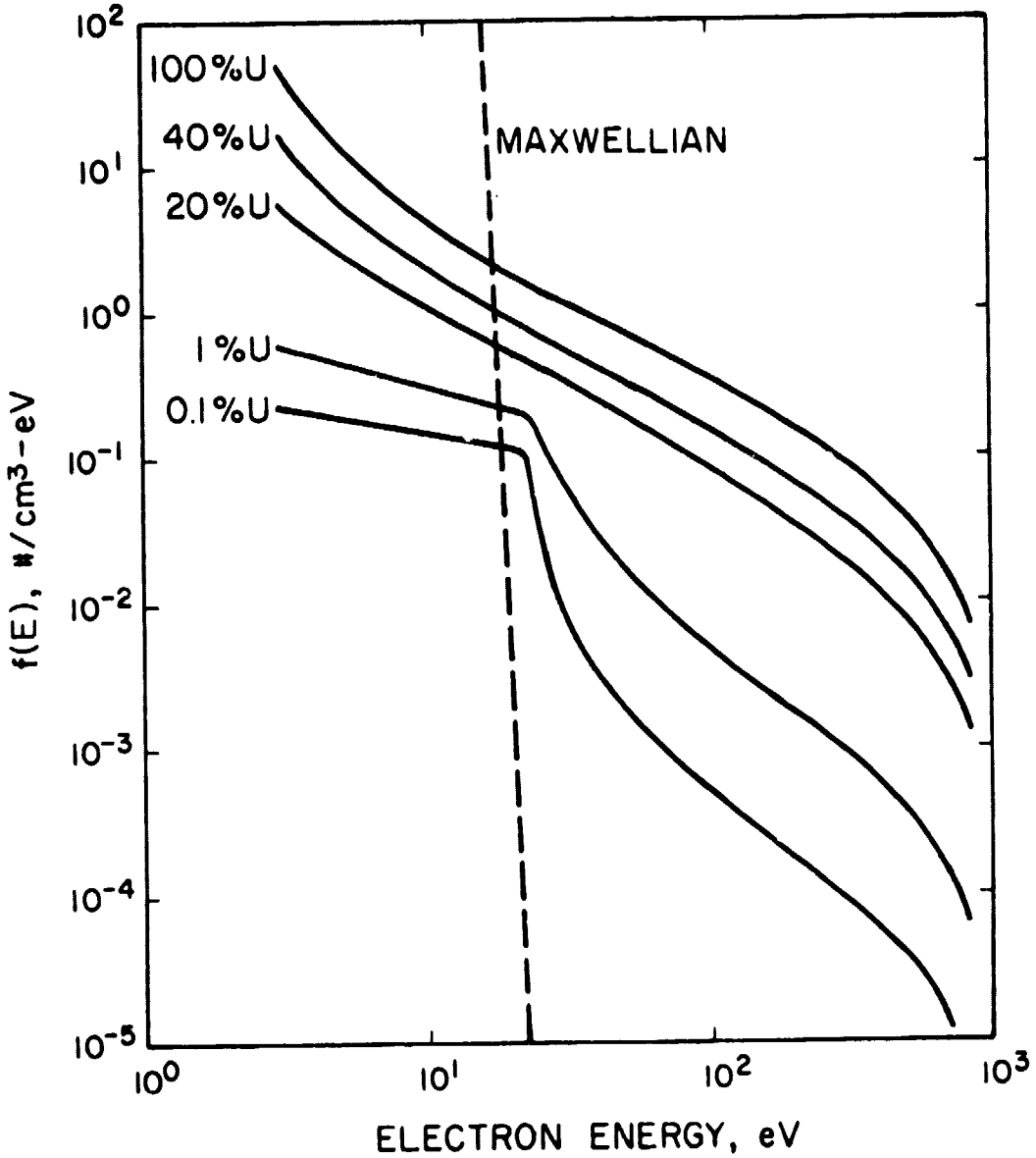

Fig. 7. High-Energy Tails for Various Concentrations of Uranium for a Plasma Temperature of 5000°K and a Neutron Flux of 2 x 10^{12}/cm^2-sec.

B. Energy Loss Curves

Figure 8 shows the rate of electron energy loss due to coulomb collisions with charged background species versus the partial pressure of uranium for three different electron energies. The energy loss is greatest for the slowest electrons and decreases with increasing energy. Also, the energy loss decreases with decreasing uranium concentration. This occurs because as the uranium concentration decreases the total number of ions decreases and since the coulomb interaction is a collective interaction the energy lost per collision decreases with the total ion density. Note that these curves closely resemble the shape of the ionization fraction of uranium shown in Fig. 5.

Figure 9 shows the ratio of the rate of electron energy loss due to collisions (other than coulomb) with He and He^+ to the total rate of energy loss versus the partial pressure of uranium.

As is evident U, U^+, and U^{++} dominate the slowing process. This occurs for two reasons. First, the threshold for excitation and ionization of U, U^+, or U^{++} is much lower than that of He. In general the smaller the energy loss the more probable the event is. Hence the probability of an electron losing energy to U, U^+, or U^{++} is greater than that of losing energy to He, or He^+. Secondly, He^+ is a minority species. Because of this its contribution to the total $\frac{dE}{dt}$ is very small. This leaves only ionization and excitation of neutral He as loss mechanisms for electrons with He.

The total rate of electron energy loss versus the partial pressure of uranium is shown in Fig. 10. An essentially linear decrease in

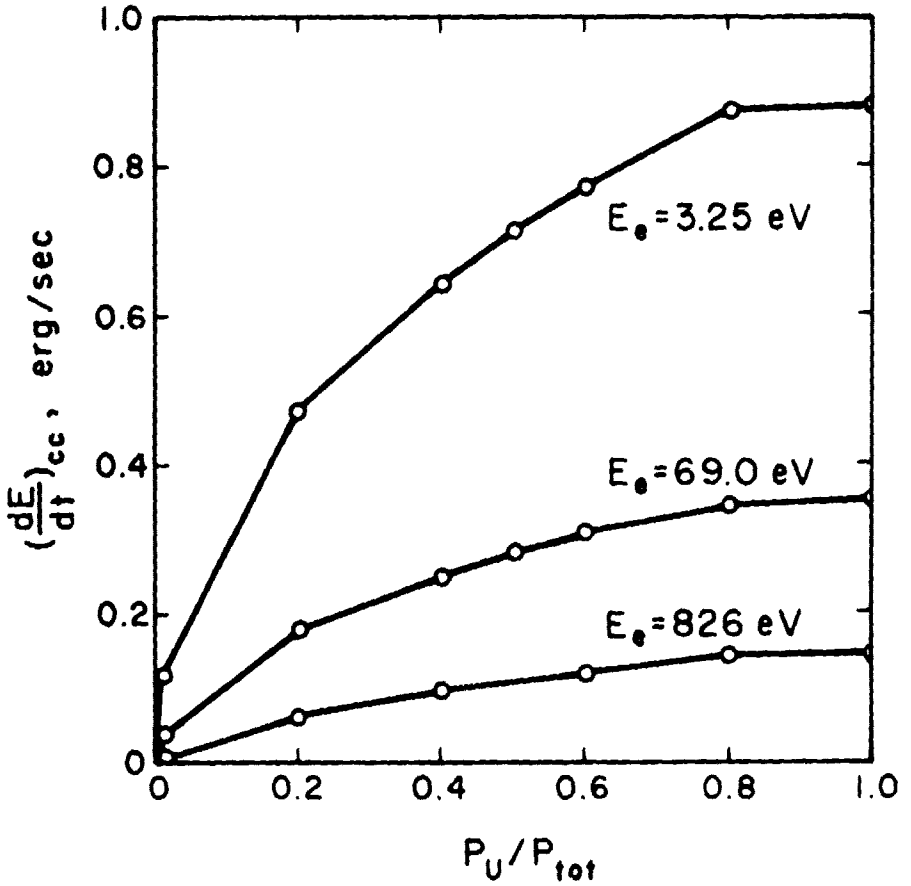

Fig. 8. $\frac{dE}{dt}$ due to Coulomb Collisions vs. Partial Pressure of U.

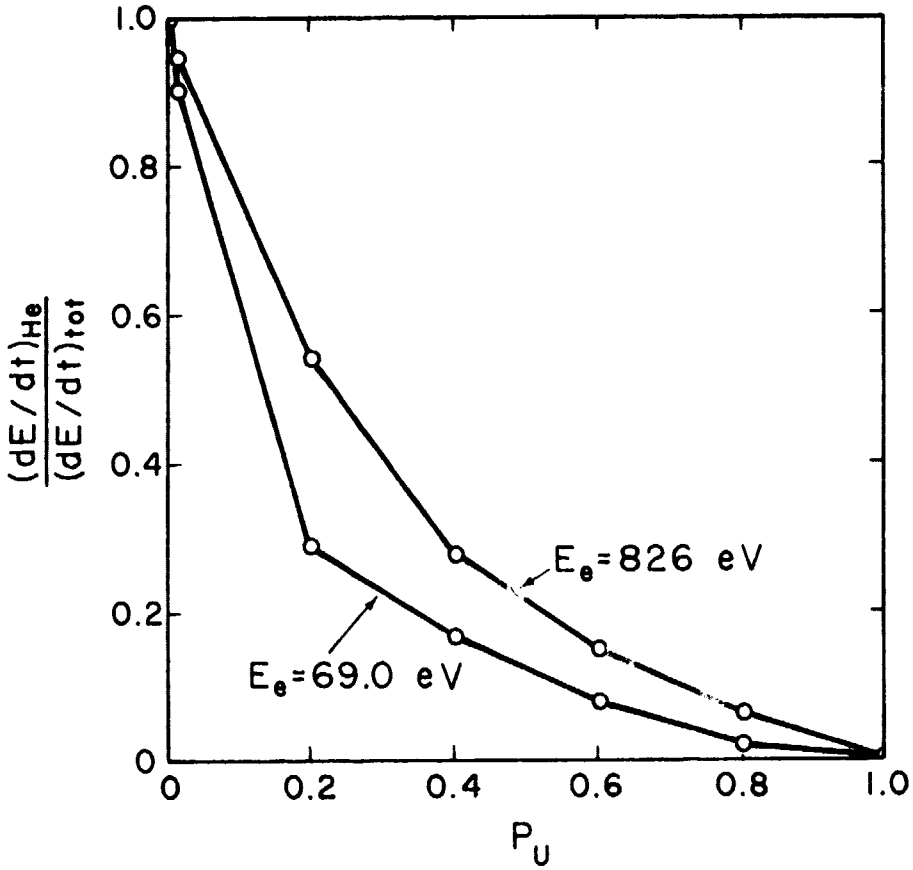

Fig. 9. Ratio of the Rate of Electron Energy Loss Due to He to the Total Rate of Energy Loss vs. the Partial Pressure of Uranium.

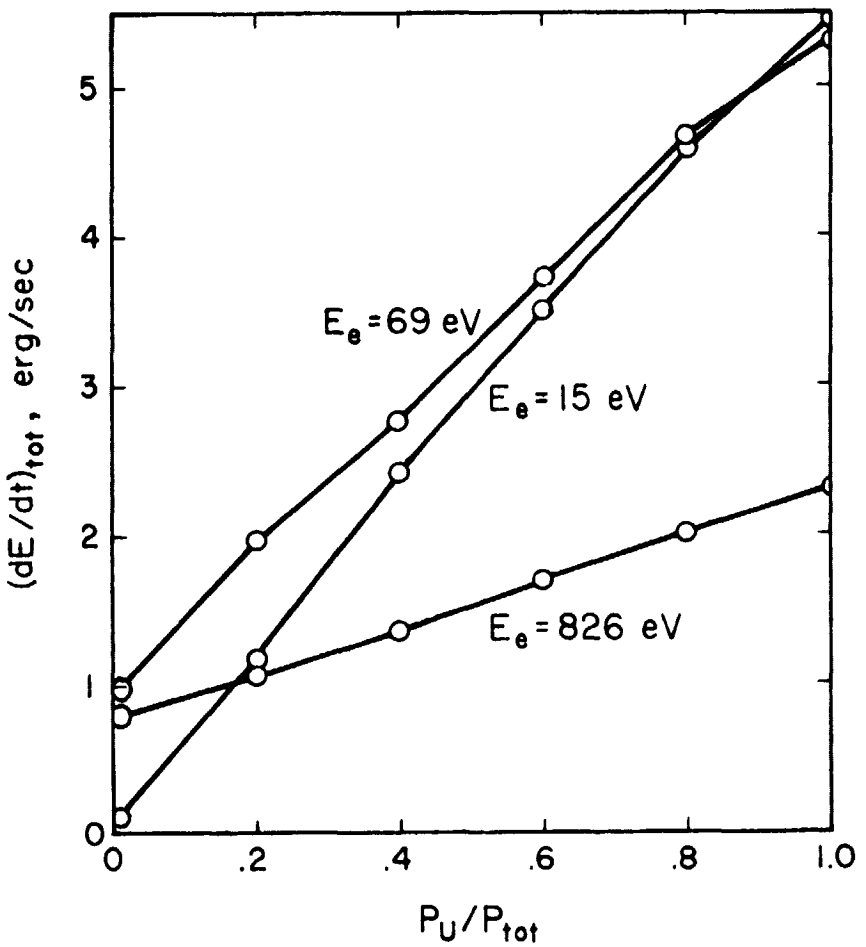

Fig. 10. Partial Pressure of U vs. Total $\frac{dE}{dt}$ for Different Electron Energies.

$\left(\frac{dE}{dt}\right)_{tot}$ with a decrease in partial pressure of uranium occurs for all three electron energies shown. Since an electron with an energy of 19.82 eV or less can neither ionize or excite He, the $\frac{dE}{dt}$ for the 15 eV electron must tend towards zero as the concentration of uranium decreases. For electron energies above 19.82 eV a nonzero limiting value of $\left(\frac{dE}{dt}\right)_{tot}$ is reached for zero concentration of uranium.

V. DISCUSSION

The accuracy of the above results are limited to how well the assumption of continuous slowing down is fulfilled and the accuracy of the cross sections used. It was necessary to use the Gryzinski cross section model for uranium although this model was developed for hydrogenic atoms. No experimental data exists which could serve as a base for comparison. However, Bathke[1] estimates the uncertainty in the theoretical cross sections is a factor of two. The accuracy is also limited in the 20 to 100 keV range by the weakening of the assumption of continuous slowing down.

The results obtained here are consistent with those of Bathke[1] in that in the limit of zero helium density his distribution is obtained.

As noted above, the density of the He-metastable state was assumed to be 10^{-4} x density of helium. The exact ratio is not crucial to the final results. If this ratio was lowered by an order of magnitude it would not change the distribution by more than .1%. Considering the uncertainty in the cross-sections this is not thought to lead to a serious error.

VI. CONCLUSION

The major reason for adding He to the uranium plasma is to take advantage of non-maxwellian excitation due to the high-energy tail. He was chosen because of its high lying excited states in the range of the non-maxwellian tail. By the same token, because of the large ionization potential of He, little of it is ionized. So by adding He to the plasma the electron population is depleted which in turn causes fewer excitations in both He and U. Thus the chances of achieving an inversion seems slim.

There are several others reasons to suspect that inversions will be difficult to achieve. One is that in a preliminary calculation performed by Maceda with a neutron flux of $2 \times 10^{16}/cm^2$-sec, a temperature of 5000°K, and 40% concentration of He, the excitation rates from ground and the two metastable states (2's and 3's) up was significantly less (10^{-4}) than the corresponding down rates. Although the possibility of achieving a laser is not excluded by this calculation, the power from such a laser would be very low as the metastable densities were calculated to be $\sim 10^8/cm^3$.

The results of this study also indicate that the species with the smaller excitation and ionization energies will dominate the slowing down of electrons. The reason is that in such cases there are more ways for the electron to slow down. For example little He is ionized so that He^+ contributes little to the coulomb $\frac{dE}{dt}$.

Of course the addition of He still improves the heat transport properties of the plasma as mentioned in the introduction. This is quite desirable in many of the applications of uranium plasmas.

VII. REFERENCES

1. C. G. Bathke, "Calculations of the Electron Energy Distribution Function in a Uranium Plasma by Analytic and Monte Carlo Techniques," Ph.D. Thesis, Nuclear Engineering Program, Univ. of Illinois, Urbana, IL (1976).

2. K. Thom and R. T. Schneider, editors, Proceedings of a Symposium, "Research on Uranium Plasmas and Their Applications," NASA SP-236, 1971 (U.S. Government Printing Office), and R. G. Ragsdale, editor, Proceedings, "2nd Symposium on Uranium Plasmas: Research and Applications," AIAA, 1971.

3. R. S. Ragsdale and E. A. Willis, "Gas-Core Rocket Reactors--A New Look," NASA TMX-67823, U. S. National Technical Information Service (1971).

4. Jon B. Panglorn, "Laboratory Investigations on Thermochemical Hydrogen Production," Conference Proceedings of 1st World Hydrogen Energy Meeting (1976).

5. J. L. Russel, et al., "Water Splitting--A Progress Report," Proceedings of 1st World Hydrogen Energy Conference (1976).

6. D. C. Majumdar, H. Reyes, and W. Kerr, "The Aqueous Homogeneous Reactor as a Source of Hydrogen and of Process Heat," Dept. of Nuclear Engineering, The Univ. of Michigan (1975).

7. R. J. DeYoung, W. E. Wells, J. T. Verdeyen and G. H. Miley, "A Direct Nuclear Pumped Ne-N_2 Laser," IEEE/OSA Conference on Laser Engineering and Applications, Washington, D. C., May 1975.

8. G. S. Jones, I. Itzkan, C. T. Pike, R. H. Levy, and L. Levin, "Two-Photon Laser Isotope Separation of Atomic Uranium: Spectroscopic Studies, Excited-State Lifetimes, and Photoionization Cross Sections," IEEE Journal of Quantum Electronics (1976).

9. J. C. Diels, "Efficient Selective Excitation for Isotope Separation, Using Short Laser Pulses," Center for Laser Studies, Univ. of Southern California, Los Angeles, CA.

10. R. Paternoster, M. J. Ohanian, R. T. Schneider and K. Thom, "Nuclear Waste Disposal Utilizing a Gaseous-Core Reactor," Trans. Am. Nucl. Soc., 19, 204 (1974).

11. J. R. Williams, J. D. Clement, and J. H. Rust, "Analysis of UF_6 Breeder Reactor Power Plants," School of Nuclear Engineering, Georgia Institute of Technology (1974).

12. R. H. Lo and G. H. Miley, "Electron Energy Distribution in a He Plasma Created by Nuclear Radiation," IEEE Transactions on Plasma Science, Vol. PS-2, December, 1974.

13. B. S. Wang, "Monte Carlo Simulation of Nonlinear Radiation Induced Plasmas," Ph.D. Thesis, Dept. of Computer Science, Univ. of Illinois, Urbana, IL (1972).

14. E. Maceda, "Line Radiation from Uranium Plasmas," Ph.D. Thesis, Nuclear Engineering Program, University of Illinois, Urbana, IL (1977).

15. D. R. Suhre, "Energy Distributions of Electrons in Electron Beam Produced Nitrogen Plasmas," Ph.D. Thesis, Electrical Engineering Program, Univ. of Illinois, Urbana, IL (1976).

16. M. Gryzinski, "Classical Theory of Electronic and Ionic Inelastic Collision," Phys. Rev., 115, 374 (1959).

17. L. Vriens, "Binary-Encounter Electron-Atom Collision Theory," Phys. Rev., 141, 88 (1966).

18. D. V. Sivukhin, "Coulomb Collisions in a Fully Ionized Plasma," Review of Plasma Physics, Vol. 4, Consultants Bureau, New York (1966).

19. Private Communication with E. Maceda.